shown that Bss HII, Eag I, Nae I and, Sac II sites are clustered in less than 2 kb in the proximal CpG-rich region, which is thus a true CpG island.

REFERENCES AND NOTES

1. R. L. Nussbaum and D. H. Ledbetter, *Annu. Rev. Genet.* **20**, 109 (1986).
2. G. R. Sutherland, *Am. J. Med. Genet.* **31**, 125 (1979); ———, E. Baker, A. Fratini, *ibid.* **22**, 433 (1985).
3. S. L. Sherman, P. A. Jacobs, N. E. Morton, U. Froster-Iskenius, P. N. Howard-Peebles, *Hum. Genet.* **69**, 289 (1985).
4. C. D. Laird, *Genetics* **117**, 587 (1987); ———, M. M. Lamb, J. L. Thorne, *Am. J. Hum. Genet.* **46**, 696 (1990).
5. A. Vincent *et al.*, *Nature* **349**, 624 (1991).
6. F. Rousseau *et al.*, *Am J. Hum. Genet.* **48**, 108 (1991).
7. B. H. Brownstein *et al.*, *Science* **244**, 1348 (1989).
8. E. D. Green and M. V. Olson, *Proc. Natl. Acad. Sci. U.S.A.* **87**, 1213 (1990).
9. H. M. Albertsen *et al.*, *ibid.*, p. 4256.
10. F. E. Abidi, M. Wada, R. D. Little, D. Schlessinger, *Genomics* **7**, 363 (1990); M. Wada *et al.*, *Am. J. Hum. Genet.* **46**, 95 (1990).
11. T. Triglia, M. G. Peterson, D. J. Kemp, *Nucleic Acids Res.* **16**, 8186 (1988). Total yeast DNA was digested to completion with Eco RV, and circularized at a concentration of 3 μg/ml with 6 U Weiss of T4 DNA ligase (Biolabs) in a volume of 20 μl. Fifteen nanograms of the ligated DNA was amplified by PCR using inverted primer pairs corresponding to the right arm or the left arm of the pYAC4 vector [D. T. Burke, G. F. Carle, M. V. Olson, *Science* **236**, 806 (1987)]. The PCR was performed in 50 μl with 2.5 U of AmpliTaq DNA polymerase (Perkin-Elmer Cetus) with the following amplification conditions: a 5-min initial denaturation at 94°C, 40 cycles of 1-min denaturation at 94°C, 1 min annealing at 60°C, 4 min elongation at 72°C (extended for 2 s per cycle) and a final elongation step of 7 min, at 72°C. The sequences of the two right arm primers were: NL10: 5′-CTCCCGGGGGCGAGTCGAACGCCCG-3′ and NL21: 5′-GCCCAGTATTCTTAACCCAACTGCACAG-3′. After amplification, the 2.9-kb fragment corresponding to the probe D53 was cloned as a 2.4-kb Eco RI–Pst I fragment in pBluescript KS+. The sequences of the two left arm primers were: NL12: 5′-CAATTAAATACTCTCGGTAGCCAAG-3′ and NL13: 5′-CCGGTCCTTCCAAGATGGTTCAGAGTG-3′. After amplification, a 1.4-kb fragment corresponding to the probe G53 was obtained and used as a LMP purified probe.
12. S. T. Warren *et al.*, *Proc. Natl. Acad. Sci. U.S.A.* **87**, 3856 (1990).
13. A. Vincent, unpublished results.
14. The PCR was performed in 50 μl with: 50 ng of a DNA pool of 400 YACs, 0.5 μg of each primers OI39 (5′-GTGAAGCAATTTGAGTTGGTGGGAG-3′) and OI41 (5′-CCCAAGTTTAGCTTCCGTAGAAGCC-3′), 2.5 U of AmpliTaq DNA polymerase with the following amplification conditions: a 5-min initial denaturation at 94°C, 35 cycles of 1-min denaturation at 94°C, 1-min annealing at 60°C, 8-min elongation at 72°C (extended for 2 s per cycle), and a final elongation step of 10 min at 72°C. Identification of YAC 141H5 from the positive YAC pool was performed by dot blot hybridization.
15. D. Heitz *et al.*, unpublished data.
16. A. P. Bird, *Trends Genet.* **3**, 342 (1987).
17. R. P. Kandpal, H. Shukla, D. C. Ward, S. M. Weissman, *Nucleic Acids Res.* **18**, 3081 (1990); A. Poustka and H. Lehrach, in *Genetic Engineering: Principles and Methods*, J. Setlow, Ed. (Plenum, New York, 1988), vol. 10, p. 169. Total yeast DNA, prepared in low melting agarose block (about 5 μg per block) was partially digested with Eag I in 1 mM $MgCl_2$ and circularized at a concentration of 200 ng/ml with 30 U Weiss of T4 DNA ligase in a volume of 1 ml. The ligase was inactivated at 68°C and 10 ng of ligated DNA was digested by Eco RI after adjusting the NaCl concentration to 100 mM. Afterwards, the enzyme was inactivated at 68°C for 20 min and DNA precipitated with NaCl, glycogen and ethanol. The digested DNA was then recircularized at a concentration of 1 ng/μl with 1.5 U Weiss of ligase in a total volume of 50 μl. Ligation product (5 ng) was amplified in 50 μl as described (*11*) in presence of right-arm-specific inverse-PCR primers NL9 and OR19 (NL9: 5′-CGAGTCGAACGCCCGATCTCAAG-3′ and OR19: 5′-GGCCATTATCGCCGGCATGG-3′). The 1.1-kb fragment corresponding to probe F33 was cloned as a 1-kb Eco RI–Eag I fragment in pBluescript KS+.
18. S. F. Wolf *et al.*, *Proc. Natl. Acad. Sci. U.S.A.* **81**, 2806 (1984); D. Toniolo *et al.*, *EMBO J.* **7**, 401 (1988).
19. P. Lichter *et al.*, *Science* **247**, 64 (1990); J. Shaw, P. Lichter, A. J. Driesel, R. Williamson, S. Chamberlain, *Cytogenet. Cell Genet.* **53**, 221 (1990).
20. C. J. Harrison, E. M. Jack, T. D. Allen, R. Harris, *J. Med. Genet.* **20**, 280 (1983).
21. E. Maestrini *et al.*, *Genomics* **8**, 664 (1990).
22. F. Rousseau, unpublished results.
23. J. A. Sved and C. D. Laird, *Am. J. Hum. Genet.* **46**, 443 (1990).
24. H. F. Willard *et al.*, *Nucleic Acids Res.* **11**, 2017 (1983).
25. V. Montanaro *et al.*, *Am. J. Hum. Genet.*, in press.
26. E. M. Southern *et al.*, *Nucleic Acids Res.* **15**, 5925 (1987).
27. R. Fujita *et al.*, *Proc. Natl. Acad. Sci. U.S.A.* **87**, 1796 (1990).

28. We wish to thank C. Kretz for her expert technical assistance, S. T. Warren for the generous gift of DNA from hybrid cell lines, and R. Tupler and C. Barletta for help in the in situ hybridization experiments. We are also grateful to G. R. Sutherland for communicating his data about XTY26 previously to publication. Supported by grants from Ministère de la Recherche et de la Technologie (87C.0397) and Caisse Nationale d'Assurances Maladie to J.L.M. from Association Française contre les Myopathies to D.C., from the Associazione Italiana per la Ricerca sul Cancro and Progetti Finalizzati CNR to G.D.V. and D.T. F.R. was supported by a postdoctoral fellowship from the Medical Research Council of Canada.

8 January 1991; accepted 8 February 1991

Subtle Cerebellar Phenotype in Mice Homozygous for a Targeted Deletion of the *En-2* Homeobox

A. L. JOYNER, K. HERRUP, B. A. AUERBACH, C. A. DAVIS, J. ROSSANT

The two mouse genes, *En-1* and *En-2*, that are homologs of the *Drosophila* segmentation gene *engrailed*, show overlapping spatially restricted patterns of expression in the neural tube during embryogenesis, suggestive of a role in regional specification. Mice homozygous for a targeted mutation that deletes the homeobox were viable and showed no obvious defects in embryonic development. This may be due to functional redundancy of *En-2* and the related *En-1* gene product during embryogenesis. Consistent with this hypothesis, the mutant mice showed abnormal foliation in the adult cerebellum, where *En-2*, and not *En-1*, is normally expressed.

TWO HIGHLY CONSERVED HOMEOBOX-containing genes, *En-1* and *En-2*, have been identified in mouse (*1*) and other vertebrates (*2–5*), based on their sequence similarity to the *Drosophila* genes, *engrailed (en)* and *invected (inv)* (*6, 7*). All *en*-like genes contain four conserved protein domains including the homeobox (Fig. 1A), suggesting that they have similar biochemical functions. The *Drosophila en* gene has been shown by mutational and mosaic analysis to be required for embryonic segmentation (*8*) and later development of the nervous system (*9*). The *En* and *inv* genes are coexpressed in a pattern consistent with these roles (*7, 10*).

Comparative expression studies have shown that in vertebrates, from zebrafish to mice, the *En* genes are expressed in a highly specific pattern in the developing embryo (*3–5, 11–14*), indicating conservation of function. During and after neural tube closure, *En-1* and *En-2* are expressed in a band of cells spanning the junction between mid- and hindbrain, apparently defining a specific spatial domain in the developing nervous system. *En-1*, unlike *En-2*, is also expressed in specific domains within the spinal cord, somites, and limbs, beginning at 9.5 days of development. In the mouse, expression of both *En* genes in the brain later becomes progressively limited to different specific groups of neurons (*11, 12*). In the adult, *En-1* and *En-2* continue to be coordinately expressed in a number of motor nuclei in the pons region and in cells within the substantia nigra. However, *En-2* alone is expressed in the granule cell layer of the cerebellum.

The two phases of *en* expression in neural development have been suggested to reflect roles in both compartmentalization of the developing neural tube and later specification of particular neuronal populations (*11*). Proof of such roles requires mutational analysis in animals. The advent of targeted mutagenesis by homologous recombination in mouse embryonic stem (ES) cells has

A. L. Joyner, C. A. Davis, J. Rossant, Division of Molecular and Developmental Biology, Samuel Lunenfeld Research Institute, Mount Sinai Hospital, 600 University Avenue, Toronto, Ontario, Canada M5G 1X5, and Department of Molecular and Medical Genetics, University of Toronto, Canada.
K. Herrup, Shriver Center for Mental Retardation Inc., 200 Trapelo Road, Waltham, MA 02254.
B. A. Auerbach, Division of Molecular and Developmental Biology, Samuel Lunenfeld Research Institute, Mount Sinai Hospital, 600 University Avenue, Toronto, Ontario, Canada M5G 1X5.

opened up the possibility of generating null mutations in cell culture, and subsequently introducing the mutations into the germline (*15*). Here we report on the germline transmission and phenotypic analysis of a mutation in the *En-2* gene that we previously produced in ES cells (*16*).

The *En-2* mutation created by homologous recombination resulted in the replacement of approximately 1 kb of the *En-2* gene, consisting of 300 bp of intron and 700 bp of the homeobox exon including the end of translation, with a 1.5-kb *neo* expression vector (*16*) (Fig. 1A). A truncated protein that contains two of the *en*-conserved domains might still be produced from the mutant locus, but, by analogy to *Drosophila* homeodomain proteins, such a protein would be predicted to have no DNA-binding activity (*17*). An intact homeodomain is required not just for DNA binding but also for gene function. In the *Drosophila* en^{IM99} mutation, the Gln codon at position 45 of the homeodomain is replaced by a termination codon (TAG). This interruption of the coding sequence grossly impairs *en* function (*18*). Furthermore, deletion of the homeodomain in the *Drosophila Antp* gene eliminates function in an in vivo ectopic expression assay (*19*).

One of the three mutant 129/Sv-derived ES cell lines generated resulted in transmission of the $En\text{-}2^{hd}$ (homeobox deletion) mutation into the germline after injection of the cells into either C57BL/6 or BALB/c blastocysts (Table 1) (*20*). The germline chimeras were bred with C57BL/6, CD1, and 129/Sv mice, producing heterozygous mutant offspring on two hybrid and one inbred (129/Sv) backgrounds. Approximately 50% of the ES-derived offspring (114 out of 217) carried the expected deletion of the *En-2* homeobox in one allele of *En-2*, as determined by Southern (DNA) blot analysis, and appeared normal. Heterozygous crosses were established and 224 offspring have been typed: 55 were wild type, 104 were heterozygous, and 65 were homozygous for the *En-2* mutation (Fig. 1B). Mice homozygous for the $En\text{-}2^{hd}$ mutation were viable on all three genetic backgrounds. Breeding pairs have been established with homozygous mice on a hybrid background, and they have produced apparently normal-sized litters. The absence of a fully functional *En-2* protein was therefore compatible with survival and reproduction. Microscopic examination of intact homozygous embryos at 8, 9, and 12 days of development revealed no signs of gross abnormalities in organization of the mid- to hindbrain region. Thus, we could find no evidence for a major effect of the mutation on embryonic development.

Immunoblot analysis was performed on protein from 9.5-day embryos and newborn and adult cerebellum with an antibody raised against the *En-2* homeobox region that cross-reacts with both *En-1* and *En-2* proteins (Fig. 2A) (*5*). This analysis detected no normal *En-2* protein in homozygous mutant tissues and showed that expression of the related *En-1* gene product was not grossly affected by the absence of *En-2*. No antibody is available that could have detected the putative truncated *En-2* protein. However, Northern blot analysis of RNA from embryos and adult tissues from mutant homozygous and heterozygous mice demonstrated the presence of a read-through transcript from the $En\text{-}2^{hd}$ locus in brain samples that might produce a truncated protein (*21*) (Fig. 1A). Continued production of such a transcript in homozygous $En\text{-}2^{hd}/En\text{-}2^{hd}$ mice suggests that transcription from the *En-2* promoter does not require expression of the *En-2* protein.

Whole-mount immunocytochemical analysis of 8.5-day and 9.5-day embryos showed that the pattern of *En-1* expression in the neural tube of homozygous mutant embryos was indistinguishable from expression of *En-1* and *En-2* in wild-type embryos (Fig. 2B). We suggest that the absence of an embryonic phenotype in $En\text{-}2^{hd}/En\text{-}2^{hd}$ mutants reflects functional redundancy between the structurally related genes, *En-1* and *En-2*, since *En-1* protein is expressed in the same embryonic domain as *En-2*. This explanation seems intrinsically more likely than the possibility that *En-2* is expressed but has no function at all in embryonic development or that a putative truncated protein product from the $En\text{-}2^{hd}$ mutant allele acts in some entirely unexpected way to restore function in vivo.

If functional redundancy between *En-1* and *En-2* is the correct explanation for the absence of an embryonic phenotype, then one would predict developmental consequences in those tissues where *En-2*, but not *En-1*, is expressed. The adult cerebellum

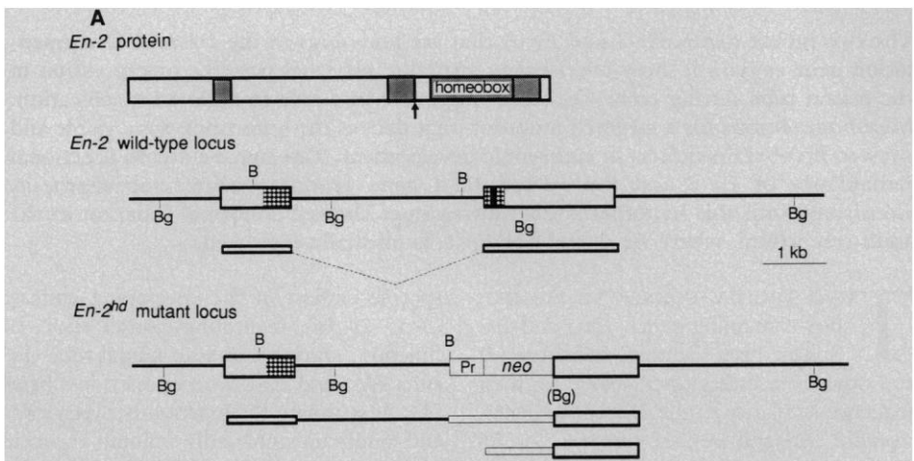

Fig. 1. (**A**) Structure of the *En-2* protein and wild-type and mutant loci. The normal *En-2* protein product is shown schematically at the top with the four *en*-conserved domains depicted as stippled boxes. The 60–amino acid homeobox is indicated. The NH_2-terminal–conserved region includes 12 amino acids found in all *en*-like genes and five additional amino acids found in vertebrate *En* genes (*32*). The conserved domains NH_2- and COOH-terminal of the homeobox are 17 and 21 amino acids, respectively. The arrow indicates the position of the intron in the *En-2* gene. The *En-2* wild-type (middle) and mutant (bottom) loci are shown schematically with the 5′ end to the left. The *En-2* exons are marked as thick-lined rectangles with the translated sequences stip-pled and the homeobox solid. The *neo*-containing vector is shown as a thin-lined rectangle and Pr indicates the 500-bp human β-actin promoter sequences (*16*). The one transcript of the wild-type *En-2* gene and two transcripts of the mutant *En-2* locus from both the *En-2* promoter and the β-actin promoter are indicated below the loci with narrow rectangles indicating the exon sequences. The restriction sites are B, Bam HI and Bg, Bgl II. (Bg) indicates the Bgl II restriction site destroyed in making the mutation. (**B**) Southern blot analysis of Bgl II–digested tail DNA from ten offspring of an $En\text{-}2^{hd}/+ \times En\text{-}2^{hd}/+$ mating probed with a DNA fragment 3′ to the homeobox (*16*). Homozygous mutant mice (−/−) contained only the 7-kb Bgl II fragment indicative of the mutant allele, whereas heterozygotes (+/−) contained both the mutant band and the 4-kb fragment from the wild-type (+/+) allele. Reprobing the blot with a cDNA probe containing sequences from the first and second exons confirmed that homozygotes were deleted for the second homeobox-containing exon. The lines to the right of the autoradiogram indicate migration of λ DNA fragments digested with Hind III.

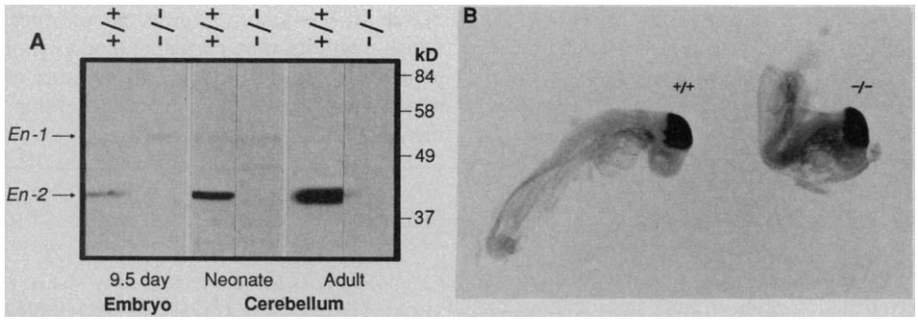

Fig. 2. *En-1* and *En-2* protein expression in *En-2*^{hd}/*En-2*^{hd} mutants. (**A**) Protein was extracted from 12 to 25 somite embryos or the tissues indicated and equivalent amounts of protein were subjected to immunoblot analysis with αEnhb-1 affinity-purified polyclonal antiserum that is specific for the homeobox region of the *En-1* (55-kD) and *En-2* (41-kD) proteins (*5*). Protein was extracted from wild-type (+/+) and *En-2*^{hd}/*En-2*^{hd} homozygous mutant animals (−/−). As expected, no cross-reacting *En-2* protein was detected in mutant tissue, but *En-1* was detected in apparently normal amounts. (**B**) Whole-mount immunohistochemical staining (*5*) with αEnhb-1 of a wild-type and an *En-2*^{hd}/*En-2*^{hd} 8.5-day embryo showed identical bands of *En* protein expression in the neural epithelium. In the wild-type embryo this expression is a composite of *En-1* and *En-2*, and in the mutant embryo it represents *En-1* protein alone. Staining of homozygous mutant and wild-type 9.5-day embryos showed the same result.

represents such a tissue in wild-type animals, and analysis of mutant cerebella, from newborn and adult mice, showed no evidence for a compensatory up-regulation of *En-1* (Fig. 2A). We therefore examined the mutant mice for signs of defects in motor control indicative of lesions in the cerebellum. Simple observation of the homozygous mutant animals (on any genetic background) did not reveal any evidence of ataxia, and the animals could perform a number of basic behavioral tests such as swimming, righting, and balancing the roller rod as well as their heterozygous and wild-type littermates. However, such assays are only a crude measure of neurological function, and need not imply normal brain function (*22*).

To determine whether the midbrain and hindbrain structures had developed properly, we removed the brains from four homozygous *En-2*^{hd}/*En-2*^{hd}, two heterozygous, and two wild-type 8-week-old mice on the inbred background. The pons, substantia nigra, and cerebellum were all present in the *En-2*^{hd}/*En-2*^{hd} homozygotes, but by gross morphological examination the cerebellum was smaller than normal, both rostro-caudally and in the mediolateral expansion of the central folia (Fig. 3, A to D). As well as this size reduction, the pattern of foliation was altered in a precise manner in all mutant animals examined. Because the pattern of cerebellar foliation varies among different inbred mouse strains (*23*), we have focused our analysis on mutant mice on the 129/Sv background, but the major alterations were consistently found in all mice whatever the genetic background. In the midline, the pattern of fissures was different in mutant and wild-type mice, with one folium (either tuber vermis or pyramis) extending uninterrupted across the entire medio-lateral plane of the cerebellar cortex. At the lateral edges, the folding patterns of Crus I and Crus II folia was altered and the extent of these lobules reduced. These changes were most apparent in lateral views (Fig. 3, C and D), where the reduction in size of the mutant paraflocculus was also apparent.

Histological analysis of serial sagittal sections revealed that all major cell types of the mutant cerebellum were present and properly positioned, and the densities of the granule cell layer and the Purkinje cell layer were not obviously different in mutant and wild-type animals (*24*) (Fig. 3E). The visual impression of reduced rostro-caudal expansion of the mutant cerebellum was supported by measurements of the length of the Purkinje cell layer in mid-sagittal sections. A mean length of 19,000 ± 1,500 μm was observed from three mutant mice examined, versus 24,100 ± 1,200 μm from three wild-type or heterozygous mice (*24*).

Further evidence of altered pattern of cerebellar folding was apparent from the

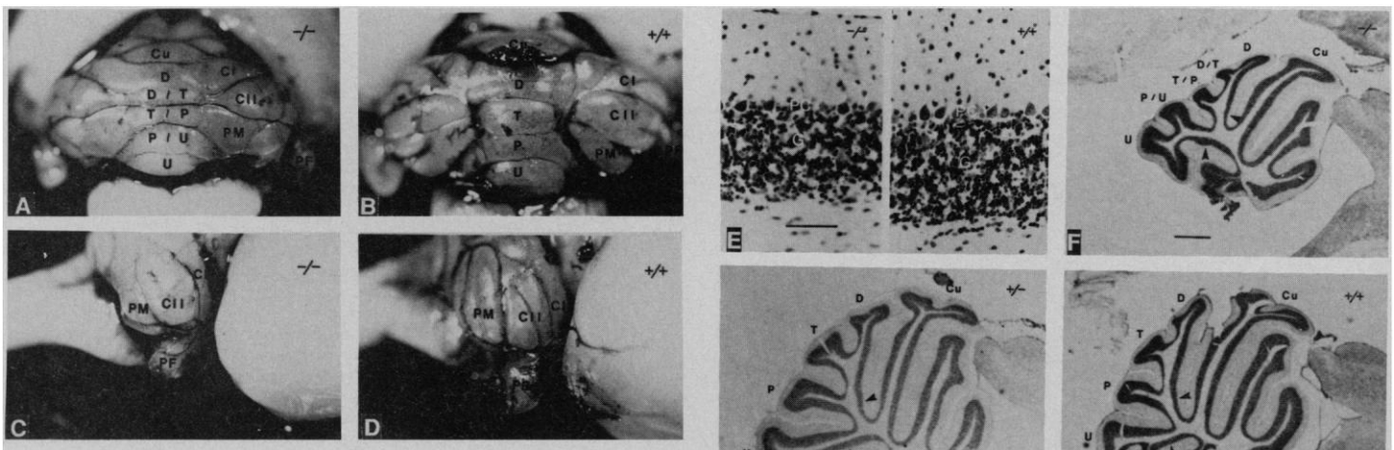

Fig. 3. Morphology and histology of *En-2*^{hd}/*En-2*^{hd} and wild-type cerebella on 129/Sv background (*33*). (**A** to **D**) Photographs of freshly dissected brains; (A and B) dorsal views, (C and D) lateral views; (A and C) *En-2*^{hd}/*En-2*^{hd} (−/−), (B and D) wild type (+/+). (**E** to **H**) Photomicrographs of sectioned material. (E) High-power magnification of part of one folium, showing normal morphology and density of Purkinje cell (PC) and granule cell layer (G) in mutant (−/−) versus wild-type (+/+) mice. The apparent small width of the granule cell layer in the mutant simply reflects that the two sections are not in completely identical regions (see F to H). Grid bar, 50 μm. (F to H) Midline sagittal sections of homozygous *En-2*^{hd}/*En-2*^{hd} (−/−, F), heterozygous *En-2*^{hd}/+ (+/−, G), and wild-type (+/+, H) cerebella. Grid bar, 500 μm for (F) to (H). Abbreviations for folia are as follows, Cu, culmen; D, declive; T, tuber vermis; P, pyramis; U, uvula; CI, Crus I; CII, Crus II; PM, paramedian lobule; and PF, paraflocculus. The alternate designation of some of the folia in the midline of the mutant cerebellum reflects uncertainty in folial assignation of the abnormal cerebellum.

histological analysis. From midline sections (Fig. 3, F to H), the patterns of foliation superficially appeared similar in mutant, heterozygous, and wild-type mice, but careful examination revealed distinct and reproducible alterations in the branching patterns of the white matter tracts that lead to the outer folia (arrows in Fig. 3, F to H). If one assumes that the outer folial shape determines folial identity, then the pattern could be interpreted as a realignment of the pyramis folium with the uvula rather than with declive and tuber vermis. However, if one assumes that the internal branching pattern, rather than the outer folial shape, is the prime indicator of folial identity, then the altered pattern in the mutant cerebellum could be interpreted as a reduction in the size of the declive, tuber vermis and pyramis lobules, and addition of an extra lobe to uvula (*25*).

Interpretation of this complex phenotype is not simple. The reduction in final size of cerebellum could be explained if *En-2* were required for overall proliferation of the granule or Purkinje cell layer, or both. However, by analogy with the reduced size but relatively normal folial patterning in midsagittal sections of mutations, such as *weaver* and *lurcher*, and animals irradiated from birth (*22, 26*), reduction in cerebellar size would not be expected to lead necessarily to altered folial patterning. There is previous evidence for genes that specifically affect cerebellar folial patterning (*23, 27*) but *En-2* is the first molecularly defined gene product shown to be involved in this process. A detailed comparison of the expression pattern of *En-2* with the ontogeny of the cerebellum in *En-2^{hd}/En-2^{hd}* mutant mice will provide more information on the mode of action of *En-2* in cerebellar development. Interactions between the *En-2^{hd}* mutation and other known cerebellar mutations may help clarify the genetic pathways involved in cerebellar patterning.

The *En-2^{hd}* mutant mice show that DNA binding activity of the *En-2* gene product is dispensable for normal embryonic development. However, the appearance of altered cerebellar foliation in mice homozygous for the *En-2^{hd}* mutation suggests that *En-2* has acquired a specialized function in the cerebellum, where during late embryonic and neonatal development *En-2* is expressed in most cells and *En-1* in only scattered groups of cells (*11, 12*). Further mutational analysis of *En-1* and *En-2* should determine whether *En-2* also has a patterning role during embryogenesis that is masked by a redundancy of function with *En-1*. The absence of gross deficiencies in development of the embryonic brain in *En-2^{hd}/En-2^{hd}* mutant mice is in contrast to the reported phenotype of mice homozygous for a mutation in the putative signaling molecule, *Wnt-1* (*28, 29*). *Wnt-1* mutant homozygotes show a deletion of a large portion of the developing brain as early as 9.5 days of development (*29*). The limits of the deletion appear to coincide with the major domain of *Wnt-1* expression at this time, a domain that overlaps almost completely with that of the *En* genes (*12, 30*). Breeding studies between *En* and *Wnt-1* mutant mice should resolve whether the mammalian *En* genes act downstream of *Wnt-1*, as occurs with their *Drosophila* homologs, *en* and *wg* (*31*). Mouse *Wnt-1* is also expressed in other regions of the developing brain and spinal cord that show no apparent defects in *Wnt-1* homozygous mutant mice, which suggests that partial redundancy of gene function may be a common feature of genes important in mammalian development.

Table 1. Chimera production with *En-2* mutant cell lines.

Cell line	Mouse strain	Blastocysts injected (no.)	Live offspring (no.)	Live chimeras (no. females, no. males)	Chimera	Offspring from chimeras	
						Non-ES-derived (no.)	ES-derived (no.)
D3	C57BL/6J	97	18	1, 7	8	34	0
					11	64	0
					12	22	0
					13	6	2
					16	2	3
					17	10	3
					18	0	0
D3-En-2-39	C57BL/6J	229	62*	7, 17	19	55	0
					20	36	0
					22	46	0
					23	41	0
					24	0	0
					28	0	67
					36	0	79
					37	39	0
D3-En-2-39	BALB/c	48	20	3, 4	1	0	113
D3-En-2-5	C57BL/6J	89	9*	0			

*In these experiments a small number of uninjected C57BL/6J embryos were transferred with the injected embryos and thus the number of live born includes uninjected embryos that survived to term.

REFERENCES AND NOTES

1. A. L. Joyner, T. Kornberg, K. G. Coleman, D. R. Cox, G. R. Martin, *Cell* **43**, 29 (1985); A. L. Joyner and G. R. Martin, *Genes Dev.* **1**, 29 (1987).
2. A. Fjose, H. G. Eiken, P. R. Njolstad, A. Molven, I. Hordvik, *FEBS Lett.* **231**, 355 (1988); C. Logan, H. F. Willard, J. M. Rommens, A. L. Joyner, *Genomics* **4**, 206 (1989).
3. C. A. Gardner, D. K. Darnell, S. J. Poole, C. P. Ordahl, K. F. Barald, *J. Neurosci. Res.* **21**, 426 (1988).
4. A. Brivanlou and R. M. Harland, *Development* **106**, 611 (1989).
5. C. A. Davis, D. P. Holmyard, K. J. Millen, A. L. Joyner, *ibid.*, in press.
6. S. J. Poole, L. M. Kauvar, B. Drees, T. Kornberg, *Cell* **40**, 37 (1985).
7. K. G. Coleman, S. J. Poole, M. P. Weir, W. C. Soeller, T. Kornberg, *Genes Dev.* **1**, 19 (1987).
8. A. Garcia-Bellido and P. Santamaria, *Genetics* **72**, 87 (1972); P. A. Lawrence and G. Morata, *Dev. Biol.* **50**, 321 (1976); T. Kornberg, *Proc. Natl. Acad. Sci. U.S.A.* **78**, 1095 (1981); P. A. Lawrence and G. Struhl, *EMBO J.* **1**, 827 (1982).
9. P. A. Lawrence and P. Johnson, *EMBO J.* **3**, 2839 (1984).
10. S. DiNardo, J. M. Kuner, J. Theis, P. H. O'Farrell, *Cell* **43**, 59 (1985); A. Fjose, W. J. McGinnis, W. J. Gehring, *Nature* **313**, 284 (1985); P. A. Ingham, A. Martinez-Arias, P. Lawrence, K. Howard, *ibid.* **317**, 634 (1985); T. Kornberg, I. Siden, P. O'Farrell, M. Simon, *Cell* **40**, 45 (1985).
11. C. A. Davis, S. E. Noble-Topham, J. Rossant, A. L. Joyner, *Genes Dev.* **2**, 361 (1988).
12. C. Davis and A. L. Joyner, *ibid.*, p. 1736.
13. D. Davidson, E. Graham, C. Sime, R. Hill, *Development* **104**, 305 (1988).
14. P. R. Njolstad and A. Fjose, *Biochem. Biophys. Res. Commun.* **157**, 426 (1988); N. H. Patel *et al.*, *Cell* **58**, 955 (1989).
15. M. R. Capecchi, *Science* **244**, 1288 (1989).
16. A. L. Joyner, W. C. Skarnes, J. Rossant, *Nature* **338**, 153 (1989).
17. C. Desplan, J. Theis, P. O'Farrell, *Cell* **54**, 1081 (1988); T. Hoey, R. Warrior, J. Manak, M. Levine, *Mol. Cell. Biol.* **8**, 4598 (1988); M. Muller *et al.*, *EMBO J.* **7**, 4299 (1988); J. Treisman, P. Gonczy, M. Vashishtha, E. Harris, C. Desplan, *Cell* **59**, 553 (1989).
18. J. W. Little and P. H. O'Farrell, personal communication.
19. G. Gibson, A. Schier, P. Lemotte, W. Gehring, *Cell* **62**, 1087 (1990).
20. All three mutant cell lines were made from the D3 129/Sv ES cell line [T. Doetschmann *et al.*, *J. Embryol. Exp. Morphol.* **87**, 27 (1985)]. Karyotype analysis at the time of freezing the lines revealed that a majority of cells in all three lines had an apparently normal male karyotype. Blastocyst injection was performed with trypsin-dissociated cells from lines maintained for no more than 4 weeks after thawing. Each blastocyst received 8 to 12 ES cells. Injected blastocysts were transferred to the uterine horns of pseudopregnant recipient females on the third day after mating with vasectomized males.
21. RNA was extracted from homozygous mutant 13.5-day embryos divided into head and body samples, and from various adult tissues (leg muscle, liver, lung, heart, kidney, spleen, forebrain, midbrain and pons, and cerebellum) of homozygous, wild-type, and heterozygous mice. RNA was analyzed by hybridization of Northern blots with a *neo* probe and *En-2* probes derived from 5′ and 3′ untranslated sequences. Two transcripts from the mutant locus (Fig. 1A) were detected in heterozygous and homozygous embryo head, adult midbrain and pons, and cerebellum tissues.
22. For example, mice heterozygous for the weaver (*Wv*/+) mutation, show abnormal cerebellar struc-

ture but no behavioral abnormality [Z. Rezai and C. H. Yoon, *Dev. Biol.* **29**, 17 (1972); D. Goldowitz and R. J. Mullen, *J. Neurosci.* **2**, 1474 (1982); K. Herrup and E. Trenkner, *Neuroscience* **23**, 871 (1987)].
23. N. Inouye and S. Oda, *J. Comp. Neurol.* **190**, 357 (1980).
24. Granule cell densities were measured from three separate areas from midline sections of two mutant, one wild-type, and one heterozygous 129/Sv mice by counting cells in a 25,000-μm^2 sample. A mean of 156 ± 22 cells per 25,000 μm^2 was recorded for the six mutant samples and 147 ± 28 for the combined heterozygous and wild-type samples. We have observed no evidence for differences between wild-type and heterozygous mice and therefore have pooled data here. The data for midline length and cell number of the Purkinje layer used to calculate Purkinje cell density were obtained from the same sections with the addition of one outbred mutant and one wild-type 129/Sv mouse. The sample size in all cases was too small for statistical analysis and reflects the small number of mice currently available on the 129/Sv inbred background. All effects described, both in overall size and cerebellar patterning, have also been observed in an equivalent number of outbred mice examined.
25. R. L. Sidman, J. B. Angevine, E. T. Taber-Pierce, *Atlas of the Mouse Brain and Spinal Cord* (Harvard Univ. Press, Cambridge, MA, 1971).
26. J. Altman and W. J. Anderson, *J. Comp. Neurol.* **146**, 355 (1972); K. W. T. Caddy and T. J. Biscoe, *Philos. Trans. R. Soc. London Ser. B.* **287**, 167 (1979).
27. P. E. Neumann, G. G. Mueller, R. L. Sidman, *Brain Res.* **524**, 85 (1990).
28. K. R. Thomas and M. R. Capecchi, *Nature* **346**, 847 (1990).
29. A. P. McMahon and A. Bradley, *Cell* **62**, 1073 (1990).
30. D. G. Wilkinson, J. A. Bailes, A. P. McMahon, *ibid.*, **50**, 79 (1987).
31. S. DiNardo, E. Sher, J. Heemskerk-Jongens, J. A. Kassis, P. H. O'Farrell, *Nature* **332**, 604 (1988); A. Martinez-Arias, N. E. Baker, P. W. Ingham, *Development* **103**, 157 (1988).
32. The *en*-conserved domains are based on sequences of the human, mouse, and chicken *En-1* and *En-2* genes (C. Logan, S. Noble-Topham, M. Hanks, A. Joyner, unpublished results) and the *Xenopus En-2* gene (A. Hemmati-Brivanlou, J. de la Torre, C. Holt, R. Harland, *Development*, in press) and *Drosophila en* and *inv* (*6*, 7). Outside of the conserved domains, only the human and mouse *En-1* or *En-2* genes show homology.
33. Brains were dissected from 2-month-old *En-2^{hd}*/*En2^{hd}*, *En-2^{hd}*/+, and +/+ mice on the 129/Sv background, which had been perfused with 4% paraformaldehyde. The brains were bisected sagittally, fixed overnight, dehydrated, cleared, and embedded in paraffin wax. Serial sagittal sections were cut at a thickness of 10 μm, mounted on subbed slides, and stained with cresyl violet.
34. We thank the various members of our laboratories for helpful discussions and support; D. Nallainathan, M. Kownacka, and C. Ung for technical assistance; H. R. Horvitz for his input on the topic of redundancies; R. Kemler for the gift of the D3 ES cell line, and J. Nadeau for the gift of 129/Sv mice. Supported by grants from the National Cancer Institute (NCI) and Medical Research Council (MRC) of Canada to A.L.J. and J.R.; from the NIH to A.L.J., J.R. (HD25334), and K.H. (NS18381 and NS20591); and from March of Dimes (1-1175) to K.H. A.L.J. is an MRC Scholar, C.A.D. is a recipient of an MRC studentship, and J.R. is a Terry Fox Cancer Research Scientist of the NCI of Canada.

4 September 1990; accepted 29 November 1990

Control of Larval Development by Chemosensory Neurons in *Caenorhabditis elegans*

CORNELIA I. BARGMANN AND H. ROBERT HORVITZ

Larval development of the nematode *Caenorhabditis elegans* is controlled by the activities of four classes of chemosensory neurons. The choice between normal development and development into a specialized larval form called a dauer larva is regulated by competing environmental stimuli: food and a dauer pheromone. When the neuron classes ADF, ASG, ASI, and ASJ are killed, animals develop as dauer larvae regardless of environmental conditions. These neurons might sense food or dauer pheromone, or both, to initiate the specialized differentiation of many cell types that occurs during dauer formation. Entry into and exit from the dauer stage are primarily controlled by different chemosensory neurons. The analysis of mutants defective in dauer formation indicates that the chemosensory neurons are active in the absence of sensory inputs and that dauer pheromone inhibits the ability of these neurons to generate a signal necessary for normal development.

THE NEMATODE *CAENORHABDITIS ELEGANS* enters one of two different life cycles after a developmental decision controlled by its nervous system. In the presence of ample food, an animal develops to adulthood through four larval stages in about 3 days (*1*). Under conditions of crowding and starvation, the development of young animals is arrested, and they differentiate into specialized larval forms called dauer larvae after the second larval molt (*2*). This alternative larval form is resistant to harsh environmental conditions, does not feed, and can survive without eating for several months. If food becomes available and the density of nematodes decreases, the dauer larva recovers to form a fertile adult.

The decision to become a dauer larva is made soon after hatching and is mediated through a competition between two chemical signals: food (usually bacteria) and a pheromone that reflects nematode density. High concentrations of pheromone and scarcity of food cause animals to enter the dauer stage (*3, 4*). This decision can be reversed at any time before or after dauer formation if food becomes available and pheromone concentrations decrease (*3, 5*).

In mutant nematodes with abnormal chemosensory neurons, dauer formation is not regulated correctly (*6, 7*). This finding suggests that the environmental stimuli that initiate dauer formation are interpreted by the nervous system. Many different cell types are subsequently altered during dauer formation, including neurons as well as hypodermal epidermal and gonadal cells that are not innervated (*8*).

The functions of particular *C. elegans* neurons can be elucidated by killing of identified cell types with a laser microbeam (*9, 10*). The nervous system of an adult hermaphrodite contains only 302 neurons, and the morphologies and synaptic specializations of all of the neurons have been reconstructed from electron micrographs of serial sections (*11*).

The amphid or phasmid sensory neurons have been implicated in the regulation of dauer formation (*6*). The cell bodies of the amphid neurons are located in ganglia in the head of the animal, and their processes run to the tip of the animal's nose, where they are exposed to the environment (*11, 12*). Each of the two amphids, one left and one right, contains eight exposed chemosensory cells: ASE, ADF, ASG, ASH, ASI, ASJ, ASK, and ADL. Two pairs of bilaterally symmetric phasmid neurons, PHA and PHB, are located in the tail.

We killed amphid and phasmid cells with a laser microbeam to assess their roles in dauer formation (*13*). When all 16 exposed amphid cells were killed in single animals, three of five animals became dauer larvae (Table 1)(*14*); when these cells and the phasmid cells were all killed, two of two animals became dauer larvae (Table 1). The animals that became dauer larvae after laser ablation were not exposed to a significant level of dauer pheromone at any point. Control animals raised under identical conditions did not become dauer larvae (Table 1).

Subsets of the chemosensory cells were killed so that the cells involved in dauer larva formation could be identified. When the amphid cells ADF, ASG, ASI, and ASJ were all killed in single animals, 30 of 37 animals became dauer larvae (Table 1). The killing of other amphid cells or phasmid cells in addition to these four cell types did not

Howard Hughes Medical Institute, Department of Biology, Massachusetts Institute of Technology, Cambridge, MA 02139.